Journal of Hazardous Materials 177 (2010) 743–749

Contents lists available at ScienceDirect

Journal of Hazardous Materials

journal homepage: www.elsevier.com/locate/jhazmat

Preparation and sono-Fenton performance of 4A-zeolite supported α-Fe_2O_3

Feng Chen*, Yan Li, Wandong Cai, Jinlong Zhang

Key Laboratory for Advanced Materials and Institute of Fine Chemicals, East China University of Science and Technology, 130 Meilong Road, Shanghai 200237, China

ARTICLE INFO

Article history:
Received 15 October 2009
Received in revised form 8 December 2009
Accepted 21 December 2009
Available online 4 January 2010

Keywords:
Sono-Fenton reaction
4A zeolite
α-Fe_2O_3
Support
Ferryl species

ABSTRACT

4A-zeolite supported α-Fe_2O_3 (Fe-4A) was prepared with a hydrothermal-calcination method, and characterized by XRD. Iron oxide in the Fe-4A composite appeared in α-Fe_2O_3 phase and was highly dispersed on the surface of 4A zeolite. Fe-4A composite effectively degraded Orange II under acidic and neutral conditions via sono-Fenton process. 4A-zeolite promoted the production of cavitation bubbles under ultrasonic treatment, while α-Fe_2O_3 promoted the homolysis of oxygen molecule producing hydroxyl radical and high-valent iron-oxo species. Both actions benefited the sono-Fenton reactivity of Fe-4A. Fe-4A-4 composite with a practical α-Fe_2O_3 content of 24.9% showed the maximum sono-Fenton reactivity to Orange II. Dissolved iron ion measurement showed that Fe-4A composite represented a low iron ion dissolution-level, while the repeatability test of recycled Fe-4A showed that Fe-4A composite has high reactivity stability and a long life-time under neutral condition in the sono-Fenton reaction.

1. Introduction

It is well known that propagation of an ultrasonic wave in an aqueous solution generates a great amount of cavitation bubbles. The cavitation bubbles then grow, pulsate, and collapse in a time range of microsecond, which leads to the formation of a hot nucleus with temperatures of thousands of degrees and pressure of hundreds of atmospheres [1]. Volatile organic compounds in the aqueous solution can easily enter the bubble and undergo direct pyrolysis within the cavitation bubble [2]. The water and oxygen molecules in the cavitation bubbles get excited and dissociate simultaneously to generate reactive species such as hydrogen atoms, hydroxyl radicals and superoxide radicals (Eqs. (1)–(4)) [3–7]:

$$H_2O \xrightarrow{\text{ultrasonic wave}} H^\bullet + {}^\bullet OH \quad (1)$$

$$O_2 \xrightarrow{\text{ultrasonic wave}} 2O^\bullet \quad (2)$$

$$O^\bullet + H_2O \rightarrow 2{}^\bullet OH \quad (3)$$

$$H^\bullet + O_2 \rightarrow HO_2{}^\bullet \quad (4)$$

All in all, water molecules and oxygen molecules dissolved in the aqueous solution and produce hydroxyl radicals and superoxide radicals under the action of ultrasonic (Eq. (5)):

$$H_2O + O_2 \rightarrow {}^\bullet OH + HO_2{}^\bullet \quad (5)$$

Previously, most wastewater treatments with ultrasonication techniques were aimed at elimination of volatile organic contaminants [2,5,7], such as halogenated organics, ethylbenzene and phenol. The degradation of the organics in the aqueous solution proceeds by direct pyrolysis in and around the collapsing bubbles and/or by oxidation by •OH. However, non-volatile organics can hardly enter the bubble and then be pyrolyzed; hence, the predominant pathway for their degradation is the •OH oxidation (Eq. (6)).

Besides reacting with organics, hydroxyl radical tends to recombine to form hydrogen peroxide (Eq. (7)) [4,8,9]. On the other hand, superoxide radical has a relatively lower activity toward organics than hydroxyl radical; hence, is more easily disproportionated to hydrogen peroxide (Eq. (8)) [4,8,9]. There is always H_2O_2 of concentrations of hundreds of micromolar presented in the aqueous solution after ultrasonication [10]. Although hydrogen peroxide itself also oxidizes organics, it reacts with hydroxyl radical and superoxide radical rapidly. As a result, sono-chemical degradation of organics usually has low reaction efficiency and results in an incomplete degradation:

$$R + {}^\bullet OH \rightarrow \text{degradation products} \quad (6)$$

$$2{}^\bullet OH \rightarrow H_2O_2 \quad (7)$$

$$2HO_2{}^\bullet \rightarrow H_2O_2 + O_2 \quad (8)$$

Fenton reaction can oxidize and degrade the organic pollutants in high efficiencies; therefore, is frequently used in wastewater treatment. However, some main disadvantages, such as high-cost from the consuming of hydrogen peroxide, pH value limitation and separation of iron ions from the treated aqueous solution,

* Corresponding author. Tel.: +86 21 6425 2062; fax: +86 21 6425 2062.
E-mail addresses: fengchen@ecust.edu.cn (F. Chen), liyan235235@sohu.com (Y. Li), jlzhang@ecust.edu.cn (W. Cai), caiwangdong1225@163.com (J. Zhang).

0304-3894/$ – see front matter © 2010 Elsevier B.V. All rights reserved.
doi:10.1016/j.jhazmat.2009.12.094

hinder the Fenton reaction from being used widely in practical applications. Many strategies have been adopted to overcome the above disadvantages, most of which involves heterogeneous Fenton system [11–15]. Iron ions were loaded to ZSM5 zeolite to make up FeZSM5 [11], or loaded to Nafion membrane to prepare a Fe-containing membrane [12,13], which show significant Fenton reactivity at neutral. A more meaningful work showed ferric phthalocyanine loaded to the ion-exchange resin presented quite good photo-Fenton reactivity in the aqueous solution [14]. The utilization of heterogeneous Fenton catalysts is promising to circumvent the pH value limitation and iron ions separation; however, high-cost from the hydrogen peroxide consuming has not been overcome.

Most improvements on the Fenton reaction involve the introduction of light or electric energy, which forms photo-Fenton and/or electro-Fenton reaction. Recently, sono-Fenton reaction combined with the ultrasonic began to appear. The iron ions in the homogeneous solution [16], or the iron oxide powders in the aqueous dispersion [17] were found to accelerate the rate of organics elimination under ultrasonic. Several recent literatures reported that heterogeneous Fenton systems under ultrasonication showed high degradation rates to organic chloride, phenol and dyes [18–21].

Several studies were even carried out without H_2O_2 addition. Pétrier reported that Fe^{2+} added into the solution enhanced the COD decrement of bisphenol A from ca. 45–80% under ultrasonic [10]. Ai also carried several studies on Fe@Fe_2O_3, which degraded nearly all of the rhodamine B and 40% of the pentachlorophenol in 60 min under ultrasonic [22,23]. Hydrogen peroxide in those studies was generated in situ via sono-chemical reactions of water and oxygen molecules. Sono-Fenton reaction is thus regarded as a potential method with ideal kinetics and alleviates the high-cost from the hydrogen peroxide consuming.

Although a detailed mechanism is still under discussion, heterogeneous materials, especially porous materials such as zeolite [24], have been confirmed significantly promoting the appearance of cavitation bubbles under the ultrasonic. The presence of heterogeneous materials induces trapped vapor gas nuclei in the crevices and pores, leading to more cavitation bubble formation [25,26]. The sono-Fenton reactivity of hematite/SBA-15 nanocomposite was thus found higher than that of unsupported iron oxides [27].

Therefore, α-Fe_2O_3 was loaded to 4A zeolite (Fe-4A) with a hydrothermal-calcination method in this work. The as-prepared Fe-4A catalyst effectively degraded an azo-dye Orange II under neutral condition via sono-Fenton process, which shows potential advantages of Fe-4A composite in sono-Fenton applications without H_2O_2 addition.

2. Materials and methods

2.1. Materials

$Fe(NO_3)_3{\cdot}6H_2O$, Na_2CO_3, $NH_4Fe(SO_4)_2{\cdot}12H_2O$, NH_4SCN, 1,10-phenanthroline and HCl were of AR and purchased from Sinopharm Chemical Reagent. Orange II was of GR and obtained from Acros Organics. Doubly distilled water was used throughout the work. Zeolite 4A was supplied by Shanghai Tianlian Fine Chemicals.

2.2. Fe-4A composite preparation

Fe-4A composite was prepared according to the literature procedure [28]. A required amount of $Fe(NO_3)_3{\cdot}6H_2O$ was dissolved into 100 mL water. Then Na_2CO_3 was slowly added into the $Fe(NO_3)_3$ aqueous solution under vigorous stirring (solution I). The amount of Na_2CO_3 added was quantified as $[Na^+]/[Fe^{3+}] = 1:1$. Meanwhile, 2.0 g 4A zeolite was dispersed into 100 mL water to form solution II. Solution I was then added dropwise into the solution II. The mixed dispersion was continuously stirred for 3 h and then transferred into a Teflon-lined stainless autoclave. The mixture was autoclaved at 120 °C for 24 h. The solid residues were centrifuged, washed with water several times, dried at 100 °C for 12 h, and then calcined at 350 °C or 500 °C for 24 h. The final obtained powder was Fe-4A composite. Pure iron oxide powder was also prepared with the same procedure as given above but without 4A zeolite and used as control.

A series of different Fe-4A composites were prepared varying the amount of Fe_2O_3 used and these samples were labeled as Fe-4A-z according to the mass ratio of $Fe(NO_3)_3{\cdot}6H_2O$ to 4A zeolite in the preparation procedure (e.g., the composite was labeled as Fe-4A-1 in the case of $Fe(NO_3)_3{\cdot}6H_2O$ mass added was 2.0 g).

Table 1
Iron oxide contents of Fe-4A composites.

Samples	Fe-4A-0.5	Fe-4A-1	Fe-4A-3	Fe-4A-4	Fe-4A-5
Practical iron oxide content[a] (%)	9.2	13.1	23.8	24.9	28.1
Theoretical iron oxide content[b] (%)	10.3	18.6	40.7	47.8	53.3

[a] Determined with ferric thiocyanate chromometry.
[b] Calculated from the quantity of $Fe(NO_3)_3{\cdot}6H_2O$ used during the preparation.

2.3. Characterization of Fe-4A composite

XRD measurements were carried out with a Rigaku D/Max 2550 VB/PC apparatus at room temperature using Cu Ka radiation (λ = 0.154056 nm) and a graphite monochromator, operated at 40 kV and 100 mA. The amount of iron oxide was measured with a ferric thiocyanate colorimetric determination [29]. 0.1 g of Fe-4A composite was refluxed in 20 mL 5.0 M HCl solution at 80 °C for 4 h. After centrifuging, the supernatant solution was mixed with 0.2 M ammonium thiocyanate in equal volumes, and diluted to an appropriate concentration for measuring. The absorbance of the solution was measured at 480 nm using a UV/vis spectrophotometer (Unico 4802) and the iron oxide content was calculated from the absorbance. The results are shown in Table 1.

2.4. Sono-Fenton reactivity measurement

All experiments were conducted in a cylindrical quartz tube (100 mL). In a typical procedure, desired concentration (10 mg/L or 20 mg/L) of Orange II was mixed with Fe-4A composite and the dispersion was stirred for 30 min. The dosage of Fe-4A was fixed at 0.5 g/L. The reaction tube was then placed into an ultrasonator (KQ2200 ultrasonic bath, operated at 40 kHz in a power of 100 W, Kunshan Ultrasonic Instruments). Reaction was timed as soon as the ultrasonator was turned on. H_2O_2 was not added throughout this work. At given reaction time intervals, 4.0 mL samples were taken out and centrifuged. The residual concentration of Orange II was then determined from the absorbance of the supernatant solution at 484 nm.

2.5. Dissolved iron ion detection

Dissolved iron ion in the aqueous solution was measured using 1,10-phenanthroline as a complexing agent [30]. The absorbance of ferrous phenanthroline at 510 nm was used to calculate the concentration of dissolved iron in the solution after sono-Fenton reaction.

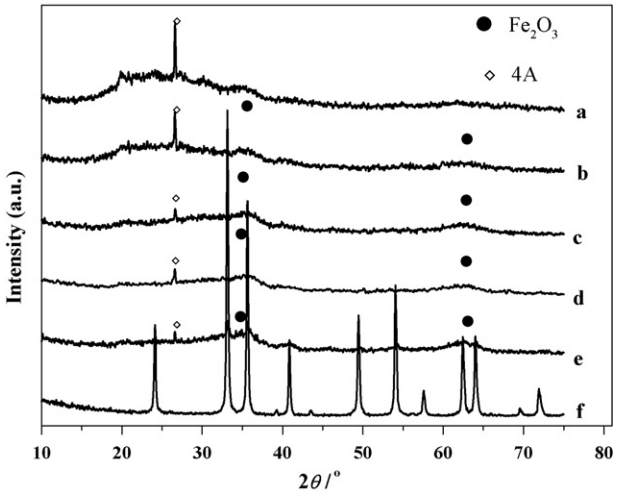

Fig. 1. XRD patterns of as-prepared iron oxide and various Fe-4A composites. (a) Fe-4A-0.5, (b) Fe-4A-1, (c) Fe-4A-3, (d) Fe-4A-4, (e) Fe-4A-5, and (f) iron oxide.

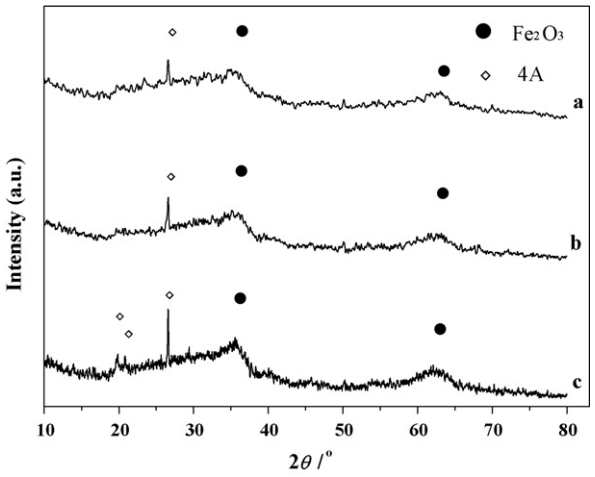

Fig. 2. The XRD patterns of Fe-4A-4 composite prepared with different procedures: (a) thermalized at 100 °C and calcined at 350 °C, (b) thermalized at 120 °C and calcined at 350 °C, and (c) thermalized at 120 °C and calcined at 500 °C.

2.6. Relative hydroxyl radical concentration detection

Hydroxyl radicals were measured by UV–vis spectroscopy in combination with the salicylic acid trapping method based on the principle of aromatic hydroxylation [31]. In a typical procedure, a salicylic acid (1.0 mM) aqueous solution was mixed with desired catalyst (in this case 0.5 g/L Fe-4A composite) in a reaction tube and stirred for 30 min. The reaction tube was then placed into the ultrasonator. After 20 min of ultrasonication, 4.0 mL samples were taken out and centrifuged. The absorbance of the supernatant solution at 510 nm was monitored to determine the concentration of hydroxyl adducts of salicylic acid, from which the relative hydroxyl radical concentration was calculated.

3. Results and discussion

3.1. Characterization of Fe-4A composite

Fig. 1 shows the XRD patterns of Fe-4A composites with different iron oxide contents and as-prepared iron oxide powder. The diffraction peaks of iron oxide powder are in agreement with the characteristic signals of α-Fe_2O_3 crystal: 24.12° (0 1 2), 33.14° (1 0 4), 35.64° (1 1 0), 40.86° (1 1 3), 49.46° (0 2 4), 54.06° (1 1 6), 57.58° (1 1 8), 62.44° (2 1 4), 64.00° (3 0 0), which undoubtedly indicated that iron oxide as-prepared was α-Fe_2O_3. As to Fe-4As, the diffraction peak at $2\theta = 26.62°$ should ascribe to 4A zeolite, while two weak broad-peaks around $2\theta = 35°$ and 63° correspond to the characteristic signal of α-Fe_2O_3. The diffractions of (1 0 4) and (1 1 0) lattice planes make up the peak around 35°, while the diffractions of (2 1 4) and (3 0 0) lattice planes make up the peak around 63°. Iron oxide in the Fe-4A composite exists in α-Fe_2O_3 phase and is highly dispersed on the surface of 4A zeolite with a small grain size. With the increase of α-Fe_2O_3 content in the Fe-4A composite, the peak intensity belonging to the 4A zeolite was greatly lowered. Besides the mass decrease of 4A zeolite in the composite, the shield effect from the α-Fe_2O_3 clusters highly dispersed on the surface of 4A zeolite to the diffraction signals of 4A zeolite should be the most possible reason.

Fig. 2 presents the XRD patterns of Fe-4A-4 prepared under various conditions. The diffraction peaks at $2\theta = 19.82°$, 20.88° and 26.62° ascribe to the characteristic signals of 4A zeolite. With the increase of hydrothermal and calcinations temperatures, the peaks around 35° and 63° were obviously increased, which means that hydrothermal and calcination favored the improvement of crystallinity of α-Fe_2O_3. Meanwhile, the diffraction peaks according to the 4A zeolite were simultaneously improved. It is most probably that the growth of α-Fe_2O_3 grain lowered its dispersibility on the surface of 4A zeolite during the hydrothermal and calcination process; and therefore, its shield effect on the X-ray diffraction of 4A zeolite was lowered, resulting in a significant increase of diffraction signals of 4A zeolite.

3.2. Sono-Fenton degradation of Orange II with Fe-4A composites

Fig. 3 gives the sono-Fenton degradation of Orange II with Fe-4A-4s prepared with various procedures. Surely, the adsorption of the Orange II on the surface of Fe-4A-4 composite was not significantly changed with the increase of the hydrothermal temperature, but significantly decreased with the increase of the calcination temperature and was also dependant on the pH value of the media. Refer to the XRD data from Fig. 2, it can be concluded that the adsorption of Orange II on the composite was achieved through an interaction between the sulfonate group and α-Fe_2O_3 cluster. At a higher calcinations temperature, the α-Fe_2O_3 cluster at the surface of Fe-4A-4 grows significantly, which lowered the total surface area of α-Fe_2O_3 clusters and thus greatly lessened the active sites for Orange II adsorption. Therefore, the adsorption of Orange II at the surface of composite was decreased from 26% to ca. 4%, as the calcinations temperature was raised from 350 to 500 °C. The isoelectric point of α-Fe_2O_3 in the aqueous solution was reported at ca. pH 6.8 [32,33], which means the surface of α-Fe_2O_3 should be positively charged under acidic condition (pH 2.7) but nearly neutral at pH 6.8. As a result, the adsorption of Orange II was greatly enhanced from pH 6.8 to pH 2.7 via an enhanced static interaction of positive charged surface of α-Fe_2O_3 and negative charged sulfonate group of Orange II. In addition, the complexing of the lone-pair electrons on the azo-bond and the electron-lack sites on the surface of composite may also have facilitated the adsorption of Orange II.

Fe-4A-4 exhibited good sono-Fenton reactivity for the degradation of Orange II under acidic and neutral conditions. At pH 6.8, the degradation ratios of Orange II with the Fe-4A-4 composites calcined at 350 °C were around 80–85%, while that with Fe-4A-4 composite calcined at 500 °C was quite decreased to a value of 43.7%. The sono-Fenton degradation of Orange II with Fe-4A-4 was lowered at pH 2.7. The degradation ratio of Orange II with Fe-4A-4 calcined at 350 °C was 76.2% and 35.1% for the composites prepared hydrothermally at 100 °C and 120 °C, respectively, while that with Fe-4A-4 calcined at 500 °C was only 10.5%. Samples calcined

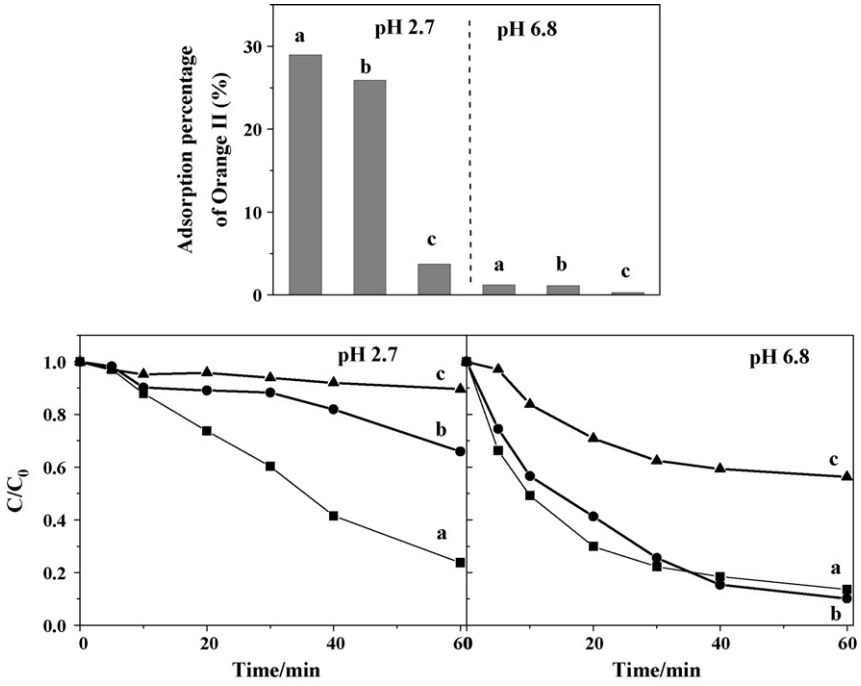

Fig. 3. Adsorption and sono-Fenton degradation of Orange II (10 mg/L) with Fe-4A-4s (0.5 g/L) prepared with different procedures: (a) thermalized at 100 °C and calcined at 350 °C, (b) thermalized at 120 °C and calcined at 350 °C, and (c) thermalized at 120 °C and calcined at 500 °C.

at 350 °C exhibited much higher reactivity than that calcined at 500 °C, which was most probably due to their larger surface area and better Orange II adsorption.

In general, the dissolved iron ions in the heterogeneous Fenton reaction would react with H_2O_2, which makes great contribution to increase the total reaction rate. Acidic condition thus favors the heterogeneous Fenton reaction as more iron ions would be dissolved into the aqueous solution under acidic condition [34]. However, Fig. 3 shows that heterogeneous sono-Fenton had higher activity under neutral condition. Therefore, the sono-Fenton reaction here is more than the simple cumulation of ultrasonic process and heterogeneous Fenton reaction. Fe-4A composites seem to catalyze the sono-chemical process in the aqueous solution, in which more reactive oxide species were produced to degrade the Orange II.

3.3. The effect of loaded content of α-Fe_2O_3 on sono-Fenton reactivity of Fe-4As

Fig. 4 shows the adsorption and sono-Fenton degradation of Orange II by Fe-4As with different α-Fe_2O_3 loaded contents. Pure α-Fe_2O_3 shows the strongest adsorption of the Orange II, which confirmed the adsorption of Orange II on the surface of Fe-4A composite relied on its interaction with α-Fe_2O_3. The loaded amount of α-Fe_2O_3 greatly affected the sono-Fenton reactivity of Fe-4A composites. The 80 min sono-Fenton degradation ratio of Orange II with Fe-4A-0.5, Fe-4A-1, Fe-4A-3 and Fe-4A-4 were 35.5%, 44.5%, 74.5% and 87.1%, respectively. However, with Fe-4A-5, the degradation ratio was lowered to 66.6%. The catalysis of α-Fe_2O_3 here was closely related to its interaction to the sono-chemical process, in which reactive species such as hydroxyl radical was generated. Therefore, the degradation rate of Orange II was mainly determined by the species and concentrations of these reactive oxide species in the sono-Fenton reaction, while these reactive oxide species relied on the amount of surface Fe^{3+} species and the cleavage rates of water and oxygen species in the hot nucleus of cavitation bubbles. Therefore, the interface between α-Fe_2O_3 clusters and the aqueous solution became very important. At the lower loaded amount of α-Fe_2O_3, the interfacial Fe^{3+} species was increased with the increase of loaded amount of α-Fe_2O_3, which catalyzed more effectively the sono-chemical degradation of Orange II. However, further increase the loaded amount of α-Fe_2O_3 did not increase the interfacial Fe^{3+} species, in stead, the Fe_2O_3 clusters grew and obviously reduce the practical amount of the interfacial Fe^{3+} species resulting in a decreased sono-Fenton reactivity. Fig. 2 shows that an obvious characteristic α-Fe_2O_3 XRD signals appears in the XRD pattern of Fe-4A-5, which suggested the appearance of α-Fe_2O_3 crystallites of larger size. Further, adsorption data in Fig. 4 also shows the interaction of Orange II with α-Fe_2O_3 grains on the Fe-4A-5 is significantly lowered than that on Fe-4A-4. Therefore, the sono-Fenton degradation reactivity of Fe-4A-5 to Orange II was weakened. The Fe-4A-4, with a practical α-Fe_2O_3 content of 24.9%, shows the maximum sono-Fenton degradation reactivity to Orange II.

Pure α-Fe_2O_3 (control) gave a sono-Fenton degradation ratio of 80.6% to Orange II in 80 min, which is quite similar with that of Fe-4A-4. However, the practical α-Fe_2O_3 contents in Fe-4As range from 9.2% to 28.1%, and hence much lower than in the pure α-Fe_2O_3. Therefore, the loading of α-Fe_2O_3 on the 4A-zeolite doubtless improves the sono-Fenton reactivity of α-Fe_2O_3.

3.4. Sono-Fenton reaction mechanism of Fe-4A catalyst

Fig. 5 presents the degradation of Orange II with various kind of catalysts under ultrasonic. Ultrasonication only in the absence of any catalyst showed little degradation to Orange II. Although ultrasonication was believed to produce reactive oxide species in the aqueous solution and thus degrade the organics, its kinetics is much slow and did not give obvious degradation to Orange II. Fe-4A-4 only without ultrasonic did not cause the degradation of Orange II. As also shown in Fig. 3, the adsorption of Orange II on Fe-4As is very weak under neutral condition. There was 18.7% of the Orange II degraded under ultrasonic in the presence of Fe^{2+}, while 18.9% of the Orange II degraded under ultrasonic in the presence of Fe^{3+} in 80 min. The pores in 4A zeolite are very small and of a size of 0.4 nm; thus, 4A zeolite is usually used as a drying agent for

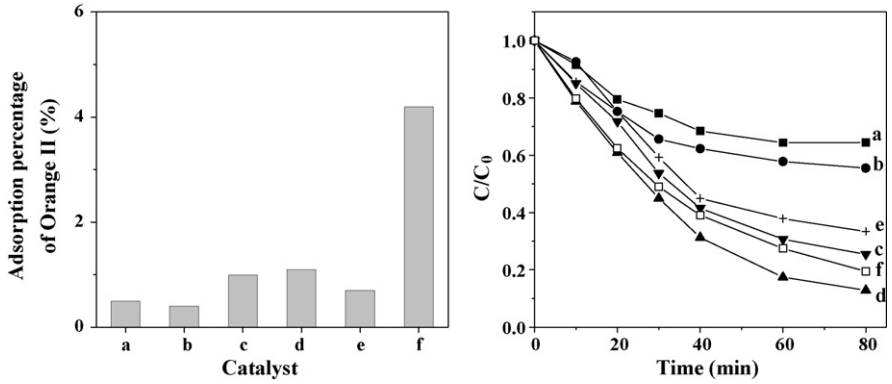

Fig. 4. Adsorption and sono-Fenton degradation of Orange II (20 mg/L) by Fe-4As (0.5 g/L) with various α-Fe_2O_3 loaded contents: (a) Fe-4A-0.5, (b) Fe-4A-1, (c) Fe-4A-3, (d) Fe-4A-4; (e) Fe-4A-5, and (f) Fe_2O_3.

solvent drying to remove water. The tunnels and pores in 4A zeolite are incapable of Orange II adsorption. After 80 min ultrasonication, only 4.8% of the Orange II was debased with 4A zeolite, which means the sono-chemical reaction in the presence of 4A zeolite was also limited for Orange II degradation. The 4A zeolite supported α-Fe_2O_3 achieved the effective sono-Fenton degradation of Orange II—gave an Orange II degradation ratio of 92.5% in 80 min.

Fe-4A presented a much higher sono-Fenton reactivity than Fe^{2+} and Fe^{3+}, which means the sono-Fenton reaction in the presence of Fe-4A would not be the simple assembly of sono-chemical process during which reactive species were produced and Fenton-reforming of reactive species by which active oxide species for organics degradation were formed; otherwise Fe^{2+} and Fe^{3+} should have exhibited higher reactivity than Fe-4As, as the optimal pH value for homogeneous Fenton reaction is around 3.0 [35]. Therefore, a synergistic reaction should have taken place in the sono-Fenton process on the surface of α-Fe_2O_3 in case of Fe-4A, in which the sono-chemical generation of reactive species and the Fenton reaction of iron species were both enhanced.

Hydroxyl radicals were measured by UV–vis spectroscopy in combination with the salicylic acid trapping method as shown in Table 2 [31]. Salicylic acid is frequently used in photocatalysis, Fenton reaction and ultrasonic studies and as a sensitive assay for •OH radical. Surely, the production of the hydroxyl radical was greatly enhanced in the presence of Fe-4A-4 under ultrasonic. In addition, 4A zeolite also promotes the generation of hydroxyl radical, which should be ascribed to the cavitation bubbling strengthening by the porous structure of 4A zeolite.

An oversimplified mechanism of sono-Fenton reaction with Fe-4A is thus proposed as follows: under sonication, highly dispersed α-Fe_2O_3 on the surface of 4A zeolite and 4A zeolite itself favors the generation of cavitation bubbles, whose pulsation and collapse produces reactive species such as hydrogen atoms, hydroxyl radicals and superoxide radicals. As reported in the literatures [25,26,36], the heterogeneous materials, especially porous materials, greatly promote the sono-chemical process; therefore, Fe-4As produce more reactive species under ultrasonic than homogeneous solution, i.e., in the presence of Fe^{2+} and/or Fe^{3+}. Contrary to the classical sono-chemical process, the reactive species mostly produced on the surface of α-Fe_2O_3 or in the pores of 4A zeolite, carried out an in situ heterogeneous Fenton reaction at the surface of α-Fe_2O_3 before they dissociated from the surface of Fe-4A composite.

In normal Fenton reaction, ferrous species are obtained via the reaction of ferric species with hydrogen peroxide [37]. However, the surface ferrous species in the heterogeneous sono-Fenton reaction here mainly produced via the reaction of surface ferric species with in situ surface generated hydrogen atom and superoxide radical (Eqs. (13) and (14)). The surface ferrous species then reacted with oxygen molecule to form a surface ferrous peroxide species, which is more under neutral condition than under acidic condition. As we know, the oxidation rate of the ferrous species in aqueous solution by O_2 is proportional to the square concentration of hydroxyl anion [38]. The ferrous peroxide species, with a weakened O–O bond, favors the homolysis to produce oxygen radicals under ultrasonic, and further hydroxyl radical and ferryl (oxidoiron(IV), Fe^{IV}=O) species (another possible pathway is ferryl species is formed via a two-electron transfer [39] before O–O bond cleavage). Alternatively, the surface ferrous species react with hydrogen

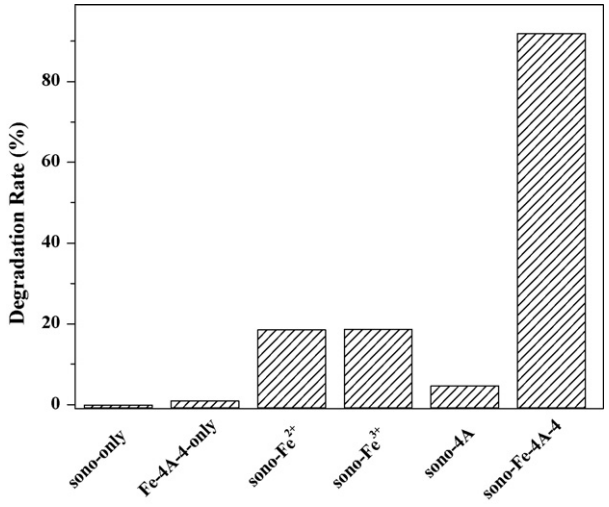

Fig. 5. Sono-Fenton degradation rate of Orange II (20 mg/L) with various kinds of catalysts (0.5 g/L) at pH 6.8 in 80 min, in the case of iron ion homogeneous solution, [Fe^{2+}] = [Fe^{3+}] = 1.6 mM, and the pH value was adjusted to ca. 2.7 to avoid the possible precipitation.

Table 2
Absorbance of the hydroxyl adducts of salicylic acid at 510 nm and corresponding relative •OH concentrations after 20 min of ultrasonic with various kinds of catalysts, pH 6.8.

	Ultrasonic only	Ultrasonic in the presence of			
		Fe^{2+}	Fe^{3+}	4A zeolite	Fe-4A-4
Absorbance	0.003	0.038	0.043	0.011	0.152
Relative •OH concentration	2.0%	25.0%	28.3%	7.2%	100%

In the cases of iron ions, [Fe^{2+}] = [Fe^{3+}] = 1.6 mM, and the pH value was adjusted to ca. 2.7.

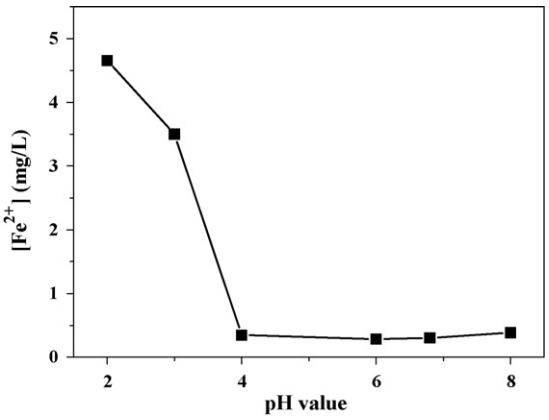

Fig. 6. Concentration of dissolved iron ion after 80 min reaction under different pH values. Fe-4A-4 0.5 g/L, [Orange II] 20 mg/L.

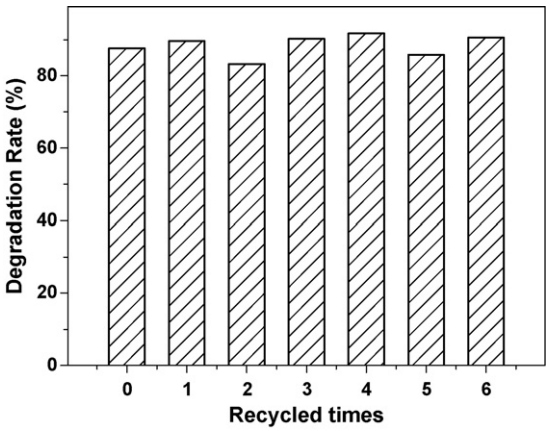

Fig. 7. Sono-Fenton degradation of Orange II with the Fe-4A-4 (0.5 g/L) of different recycled times. Reaction time 80 min, [Orange II] 20 mg/L, pH 6.8.

peroxide to produce hydroxyl radical [28]. Hydroxyl radical and ferryl species then react with Orange II and oxide it:

$$\text{ultrasonic radiation} \xrightarrow[\text{4A zeolite}]{\alpha\text{-}Fe_2O_3} \text{intensified cavitation bubble at the surface } (CB_{surf}) \quad (9)$$

$$H_2O_{ads} \xrightarrow{CB_{surf}} {}^{\bullet}H_{ads} + {}^{\bullet}OH_{ads} \quad (10)$$

$${}^{\bullet}H_{ads} + O_2 \rightarrow HO_2{}^{\bullet}{}_{ads} \quad (11)$$

$$O_2 \xrightarrow{CB_{surf}} 2O^{\bullet} \quad (12)$$

$$\equiv Fe^{3+}\text{–}OH + {}^{\bullet}H_{ads} \rightarrow \equiv Fe^{2+} + H_2O \quad (13)$$

$$\equiv Fe^{3+}\text{–}OH + {}^{\bullet}HO_{2ads} \rightarrow \equiv Fe^{2+} + H_2O + O_2 \quad (14)$$

$$\equiv Fe^{2+} + O_2 \rightarrow \equiv Fe^{2+}(O_2) \quad (15)$$

$$\equiv Fe^{2+}(O_2) \xrightarrow{CB_{surf}} \equiv Fe^{2+}\text{–}O^{\bullet} \xrightarrow{+H_2O} \equiv Fe^{4+}{=}O + 2\,{}^{\bullet}OH \quad (16)$$

$$\equiv Fe^{2+} + H_2O_2 \rightarrow \equiv Fe^{3+}\text{–}OH + {}^{\bullet}OH \quad (17)$$

$${}^{\bullet}OH + \text{OrangeII} \rightarrow \text{degradation products} \quad (18)$$

$$\equiv Fe^{4+}{=}O + \text{OrangeII} \rightarrow \equiv Fe^{3+}\text{–}OH + \text{degradation products} \quad (19)$$

3.5. Dissolved iron ion measurement and repeatability test of the Fe-4A composite

Because of the complex of the electron-rich intermediates, a main drawback of iron oxide in the heterogeneous Fenton reaction is the dissolving of iron ions and the subsequent catalyst ineffectiveness. Fig. 6 shows that the iron ion dissolution in sono-Fenton reaction was serious under acidic condition. Dissolved iron ion concentration reached 4.6 and 3.5 mg/L at pH 2.0 and 3.0, respectively. With the increase of pH value, the amount of dissolved iron ions rapidly decreased. The dissolved iron ion concentration was less than 0.40 mg/L at a pH value equals or higher than 4.0. It seems Fe-4A has a quite long life-time in sono-Fenton reaction at neutral.

Fig. 7 presents the sono-Fenton reactivity of Fe-4A-4 after recycled for several times. The reactivity of Fe-4A-4 composite was almost unchanged after recycled 7-times. The degradation percentages of Orange II were kept at 87.0 ± 5.0% in all 7 cycles. Surely, since the reaction was carried out under neutral, the dissolution of the iron ion was limited to a very low level. Thus, Fe-4A-4 composite showed high reactivity stability and a long life-time. Besides, as the sono-Fenton reaction mainly proceeds on the surface of α-Fe_2O_3 cluster, the reaction rate relies more on the surface area but not the mass of α-Fe_2O_3, which may also play a role in stabilizing the reactivity of Fe-4A-4.

4. Conclusions

Fe-4A was prepared with a hydrothermal-calcination method, which effectively degraded Orange II under acidic and neutral conditions via sono-Fenton process. Iron oxide in the Fe-4A composite is highly dispersed on the surface of 4A zeolite in α-Fe_2O_3 phase. Fe-4A composite promotes the sono-Fenton reaction by producing more cavitation bubbles under ultrasonic and catalytic homolyzing oxygen molecule to produce hydroxyl radical and high-valent iron-oxo species. The catalysis of Fe-4A composite in sono-Fenton reaction is dependant on the surface area of α-Fe_2O_3. Fe-4A-4 composite, with a practical α-Fe_2O_3 content of 24.9%, shows the maximum sono-Fenton reactivity to Orange II. Fe-4A composite showed a low iron ion dissolution-level, high reactivity stability and a long life-time under neutral condition in the sono-Fenton reaction.

Acknowledgment

This work was supported by the National Science Foundation of China (20777015) and National Basic Research Program of China (2010CB732306, 2007CB613301). We thank Ms Segomotso Bagwasi for grammar correction.

References

[1] A. Henglein, Sonochemistry: historical developments and modern aspects, Ultrasonics 25 (1987) 6–16.
[2] I. Hua, M.R. Hoffmann, Kinetics and mechanism of the sonolytic degradation of CCl_4: intermediates and byproducts, Environ. Sci. Technol. 30 (1996) 864–871.
[3] K. Makino, M.M. Mossoba, P. Riesz, Chemical effects of ultrasound on aqueous solutions. Formation of hydroxyl radicals and hydrogen atoms, J. Phys. Chem. 87 (1983) 1369–1377.
[4] P. Riesz, D. Berdahl, C.L. Christman, Free radical generation by ultrasound in aqueous and nonaqueous solutions, Environ. Health Persp. 64 (1985) 233–252.
[5] C. Pétrier, D. Casadonte, in: T.J. Mason, A. Tiehm (Eds.), Advances in Sonochemistry, Ultrasound in Environmental Protection, vol. 6, JAI Press Inc., Stamford, 2001, pp. 91–109.
[6] K. Makino, M.M. Mossoba, P. Riesz, Chemical effects of ultrasound on aqueous solutions. Evidence for hydroxyl and hydrogen free radicals (•OH and •H) by spin trapping, J. Am. Chem. Soc. 104 (1982) 3537–3539.
[7] C.G. Joseph, G.L. Puma, A. Bono, D. Krishnaiah, Sonophotocatalysis in advanced oxidation process: a short review, Ultrason. Sonochem. 16 (2009) 583–589.
[8] A. Weissler, Formation of hydrogen peroxide by ultrasonic waves: free radicals, J. Am. Chem. Soc. 81 (1959) 1077–1081.
[9] E.J. Hart, A. Henglein, Free radical and free atom reactions in the sonolysis of aqueous iodide and formate solutions, J. Phys. Chem. 89 (1985) 4342–4347.

[10] R.A. Torres, C. Pétrier, E. Combet, F. Moulet, C. Pulgarin, Bisphenol A mineralization by integrated ultrasound-UV-iron (II) treatment, Environ. Sci. Technol. 41 (2007) 297–302.
[11] H. Kušić, N. Koprivanac, I. Selanec, Fe-exchanged zeolite as the effective heterogeneous Fenton-type catalyst for the organic pollutant minimization: UV irradiation assistance, Chemosphere 65 (2006) 65–73.
[12] D. Gumy, P. Fernández-Ibáñez, S. Malato, C. Pulgarin, O. Enea, J. Kiwi, Supported Fe/C and Fe/Nafion/C catalysts for the photo-Fenton degradation of orange II under solar irradiation, Catal. Today 101 (2005) 375–382.
[13] T. Yuranova, O. Enea, E. Mielczarski, J. Mielczarski, P. Albers, J. Kiwi, Fenton immobilized photo-assisted catalysis through a Fe/C structured fabric, Appl. Catal. B 49 (2004) 39–50.
[14] M.M. Cheng, W.H. Ma, J. Li, Y.P. Huang, J.C. Zhao, Y.X. Wen, Y.M. Xu, Visible-light-assisted degradation of dye pollutants over Fe(III)-loaded resin in the presence of H_2O_2 at neutral pH values, Environ. Sci. Technol. 38 (2004) 1569–1575.
[15] S. Papic, D. Vujevic, N. Koprivanac, D. Sinko, Decolourization and mineralization of commercial reactive dyes by using homogeneous and heterogeneous Fenton and UV/Fenton processes, J. Hazard. Mater. 164 (2009) 1137–1145.
[16] I. Ioan, S. Wilson, E. Lundanes, A. Neculai, Comparison of Fenton and sono-Fenton bisphenol A degradation, J. Hazard. Mater. 142 (2007) 559–563.
[17] M. Muruganandham, J.S. Yang, J.J. Wu, Effect of ultrasonic irradiation on the catalytic activity and stability of goethite catalyst in the presence of H_2O_2 at acidic medium, Ind. Eng. Chem. Res. 46 (2007) 691–698.
[18] B. Neppolian, J.S. Park, H. Choi, Effect of Fenton-like oxidation on enhanced oxidative degradation of para-chlorobenzoic acid by ultrasonic irradiation, Ultrason. Sonochem. 11 (2004) 273–279.
[19] D.H. Bremner, R. Molina, F. Martinez, J.A. Melero, Y. Segura, Degradation of phenolic aqueous solutions by high frequency sono-Fenton systems (US-Fe_2O_3/SBA-15-H_2O_2), Appl. Catal. B 90 (2009) 380–388.
[20] Y. Segura, R. Molina, F. Martinez, J.A. Melero, Integrated heterogeneous sono-photo Fenton processes for the degradation of phenolic aqueous solutions, Ultrason. Sonochem. 16 (2008) 417–424.
[21] H. Zhang, H. Fu, D.B. Zhang, Degradation of C.I. acid orange 7 by ultrasound enhanced heterogeneous Fenton-like process, J. Hazard. Mater. 172 (2009) 654–660.
[22] Z.H. Ai, L. Lu, J.P. Li, L.Z. Zhang, J.R. Qiu, M.H. Wu, Fe@Fe_2O_3 core–shell nanowires as iron reagent. 1. Efficient degradation of rhodamine B by a novel sono-Fenton process, J. Phys. Chem. C 111 (2007) 4087–4093.
[23] Z.H. Ai, L. Lu, J.P. Li, L.Z. Zhang, J.R. Qiu, M.H. Wu, Fe@Fe_2O_3 core–shell nanowires as the iron reagent. 2. An efficient and reusable sono-Fenton system working at neutral pH, J. Phys. Chem. C 111 (2007) 7430–7436.
[24] S. Fındık, G. Gündüz, Sonolytic degradation of acetic acid in aqueous solutions, Ultrason. Sonochem. 14 (2007) 157–162.
[25] Y.Z. Dai, F.F. Li, F. Ge, F. Zhu, L.Y. Wu, X.Z. Yang, Mechanism of the enhanced degradation of pentachlorophenol by ultrasound in the presence of elemental iron, J. Hazard. Mater. 137 (2006) 1424–1429.
[26] J.K. Kim, F. Martinez, I.S. Metcalfe, The beneficial role of use of ultrasound in heterogeneous Fenton-like system over supported copper catalysts for degradation of p-chlorophenol, Catal. Today 124 (2007) 224–231.
[27] F. Martínez, G. Calleja, J.A. Melero, R. Molina, Heterogeneous photo-Fenton degradation of phenolic aqueous solutions over iron-containing SBA-15 catalyst, Appl. Catal. B 60 (2005) 181–190.
[28] J.Y. Feng, X.J. Hu, P.L. Yue, Novel bentonite clay-based Fe-nanocomposite as a heterogeneous catalyst for photo-Fenton discoloration and mineralization of orange II, Environ. Sci. Technol. 38 (2004) 269–275.
[29] American Public Health Association, Standard Methods for the Examination of Water and Wastewater Treatment, 20th ed., American Public Health Association, Washington, DC, USA, 1998.
[30] H. Tamura, K. Goto, T. Yotsuyanagi, M. Nagayama, Spectrophotometric determination of iron(II) with 1,10-phenanthroline in the presence of large amounts of iron(III), Talanta 21 (1974) 314–318.
[31] C.C. Chiueh, G. Krishna, P. Tulsi, T. Obata, K. Lang, S.J. Huang, D.L. Murphy, Intracranial microdialysis of salicylic acid to detect hydroxyl radical generation through dopamine autoxidation in the audate nucleus: effects of MPP^+, Free Radic. Biol. Med. 13 (1992) 581–583.
[32] M. Kosmulski, The pH-dependent surface charging and the points of zero charge, J. Colloid Interface Sci. 253 (2002) 77–87.
[33] M. Kosmulski, pH-dependent surface charging and points of zero charge II. Update, J. Colloid Interface Sci. 275 (2004) 214–224.
[34] J.Y. Feng, X.J. Hu, P.L. Yue, Discoloration and mineralization of orange II using different heterogeneous catalysts containing Fe: a comparative study, Environ. Sci. Technol. 38 (2004) 5773–5778.
[35] E. Neyens, J. Baeyens, A review of classic Fenton's peroxidation as an advanced oxidation technique, J. Hazard. Mater. B 98 (2003) 33–50.
[36] L.A. Crum, Comments on the evolving field of sonochemistry by a cavitation physicist, Ultrason. Sonochem. 2 (1995) 147–152.
[37] F. Chen, W.H. Ma, J.J. He, J.C. Zhao, Fenton degradation of malachite green catalyzed by aromatic additives, J. Phys. Chem. A 106 (2002) 485–9490.
[38] B. Faust, in: G.R. Helz, R.G. Zepp, D.G. Crosby (Eds.), Aquatic and Surface Photochemistry, Lewis Publishers/CRC Press, Boca Raton, FL, 1994, pp. 3–39.
[39] C.R. Keenan, D.L. Sedlak, Factors affecting the yields of oxidants from the reaction of nanoparticulate zero-valent iron and oxygen, Environ. Sci. Technol. 42 (2008) 1262–1267.